

Manuscript version: Author's Accepted Manuscript

The version presented in WRAP is the author's accepted manuscript and may differ from the published version or Version of Record.

Persistent WRAP URL:

<http://wrap.warwick.ac.uk/70883>

How to cite:

Please refer to published version for the most recent bibliographic citation information. If a published version is known of, the repository item page linked to above, will contain details on accessing it.

Copyright and reuse:

The Warwick Research Archive Portal (WRAP) makes this work by researchers of the University of Warwick available open access under the following conditions.

© 2018 Elsevier. Licensed under the Creative Commons Attribution-NonCommercial-NoDerivatives 4.0 International <http://creativecommons.org/licenses/by-nc-nd/4.0/>.



Publisher's statement:

Please refer to the repository item page, publisher's statement section, for further information.

For more information, please contact the WRAP Team at: wrap@warwick.ac.uk.

1 **Characteristics of starch-based films with different amylose contents**
2 **plasticised by 1-ethyl-3-methylimidazolium acetate**

3

4 Fengwei Xie ^{a,*}, Bernadine M. Flanagan ^b, Ming Li ^b, Rowan W. Truss ^c, Peter J. Halley ^{a,c},
5 Michael J. Gidley ^b, Tony McNally ^d, Julia L. Shamshina ^e, Robin D. Rogers ^e

6

7 ^a *Australian Institute for Bioengineering and Nanotechnology, The University of Queensland,*
8 *Brisbane, Qld 4072, Australia*

9 ^b *Centre for Nutrition and Food Sciences, Queensland Alliance for Agriculture and Food*
10 *Innovation, The University of Queensland, Hartley Teakle Building, St Lucia, Qld 4072, Australia*

11 ^c *School of Chemical Engineering, The University of Queensland, Brisbane, Qld 4072, Australia*

12 ^d *International Institute for Nanocomposites Manufacturing (IINM), WMG, University of*
13 *Warwick, CV4 7AL, UK*

14 ^e *Center for Green Manufacturing and Department of Chemistry, The University of Alabama,*
15 *Tuscaloosa, AL 35487, USA*

16

* Corresponding author. Tel.: +61 7 3346 3199; fax: +61 7 3346 3973.

Email address: f.xie@uq.edu.au, fwhsieh@gmail.com (F. Xie).

17 **ABSTRACT**

18 Starch-based films plasticised by an ionic liquid, 1-ethyl-3-methylimidazolium
19 acetate ([Emim][OAc]), were prepared by a simple compression moulding process,
20 facilitated by the strong plasticisation effect of [Emim][OAc]. The effects of amylose
21 content of starch (regular vs. high-amylose maize) and relative humidity (RH) during
22 ageing of the samples on a range of structural and material characteristics were
23 investigated. Surprisingly, plasticisation by [Emim][OAc] made the effect of amylose
24 content insignificant, contrary to most previous studies when other plasticisers were used.
25 In other words, [Emim][OAc] changed the underlying mechanism responsible for
26 mechanical properties from the entanglement of starch macromolecules (mainly
27 amylose), which has been reported as a main responsible factor previously. The
28 crystallinity of the plasticised starch samples was low and thus was unlikely to have a
29 major contribution to the material characteristics, although the amylose content impacted
30 on the crystalline structure and the mobility of amorphous parts in the samples to some
31 extent. Therefore, RH conditioning and thus the sample water content was the major
32 factor influencing the mechanical properties, glass transition temperature, and electrical
33 conductivity of the starch films. This suggests the potential application of ionic liquid–
34 plasticised starch materials in areas where the control of properties by environmental RH
35 is desired.

36

37 *Keywords:*

38 Starch; Ionic liquid; 1-Ethyl-3-methylimidazolium acetate; Plasticization;

39 Amylose/amylopectin ratio; Relative Humidity; Electrical Conductivity

40

41 Chemical compounds studied in this article

42 Starch (PubChem CID: 24836924); Water (PubChem CID: 962); Glycerol (PubChem

43 CID: 753); 1-Ethyl-3-methylimidazolium acetate (PubChem CID: 11658353)

44

45 **1. Introduction**

46 In recent years, great attention has been focused on polymers from renewable
47 resources (biopolymers: cellulose, starch, chitosan, chitin, etc.; bio-based polymers:
48 poly(lactic acid) (PLA), polyhydroxyalkanoates (PHA), etc.) due to their availability,
49 renewability, biocompatibility, and biodegradability (Yu, Dean, & Li, 2006). Among
50 these groups of polymers, starch grows in plants and is naturally structured in a
51 hierarchical multi-level complex form: from macro-observation, starch is in the form of
52 granules (<1 μm ~100 μm); many granules are broadly composed of alternating
53 amorphous and semicrystalline shells (growth rings) (100~400 nm); the semicrystalline
54 shell is stacked crystalline and amorphous lamellae (periodicity) (9~10 nm); with all
55 structures based on two major biomacromolecules called amylose (mainly linear) and
56 amylopectin (hyper-branched) (~nm) (Fu, Wang, Li, Wei, & Adhikari, 2011; Jane, 2009;
57 Pérez, Baldwin, & Gallant, 2009; Pérez & Bertoft, 2010). For the utilisation of starch, it
58 is important to understand this complex structure and how it can be altered to achieve
59 desired forms (e.g. a plasticised form).

60 With a plasticiser and elevated temperature, a process known as “gelatinisation” (with
61 abundant plasticiser content) or “melting” (with limited plasticiser content) occurs,
62 resulting in disruption of the 3D structure of native starch; and, if preferential conditions

63 are reached, this can result in a homogeneous amorphous material known as
64 “thermoplastic starch” or “plasticised starch”, which is essential in the production of
65 some starch-based materials (Avérous, 2004; Liu, Xie, Yu, Chen, & Li, 2009a; Xie,
66 Halley, & Avérous, 2012; Xie, Pollet, Halley, & Avérous, 2013). While water is the
67 most commonly used plasticiser for starch, substances such as polyols (glycerol, glycol,
68 sorbitol, etc.), compounds containing nitrogen (urea, ammonium derived, amines), and
69 citric acid have also been reported to be effective in the plasticisation of starch (Liu et al.,
70 2009a; Xie et al., 2012). A plasticiser for starch should preferably be stable (non-volatile)
71 both during thermal processing and in post-processing stages, be ineffective in starch
72 macromolecular degradation, be safe to humans and the environment, and be able to
73 provide starch-based materials with enhanced performance and new capabilities.
74 Unfortunately, the currently-used plasticisers do not yet have all the desired attributes and
75 thus finding alternative and better plasticisers for starch is of interest.

76 Ionic liquids, often referred to as “green solvents”, have the capability of dissolving
77 many substances, including many organic polymers, and have good properties such as
78 chemical and thermal stability, low vapour pressure, and high ionic activity (Lu, Yan, &
79 Texter, 2009). Many ILs, especially ones based on the imidazolium cation, have been
80 shown to be capable of dissolving polysaccharides such as starch (Biswas, Shogren,
81 Stevenson, Willett, & Bhowmik, 2006; El Seoud, Koschella, Fidale, Dorn, & Heinze,
82 2007; Wilpiszewska & Szychaj, 2011; Zakrzewska, Bogel-Lukasik, & Bogel-Lukasik,
83 2010; Zhu et al., 2006), cellulose (Heinze, Schwikal, & Barthel, 2005; Zhang, Wu, Zhang,
84 & He, 2005), chitin/chitosan (Wu, Sasaki, Irie, & Sakurai, 2008; Xie, Zhang, & Li, 2006),
85 silk fibroin (Phillips et al., 2004; Wang, Chen, Yang, & Shao, 2012; Wang, Yang, Chen,

86 & Shao, 2012), lignin (Pu, Jiang, & Ragauskas, 2007), zein protein (Biswas et al., 2006),
87 wool keratin (Xie, Li, & Zhang, 2005); and thus can be used as excellent media for
88 polysaccharide plasticisation and modification. Moreover, the use of ILs may also allow
89 for the development of starch-based ionically conducting polymers or solid polymer
90 electrolytes (Liew, Ramesh, Ramesh, & Arof, 2012; Ramesh, Liew, & Arof, 2011;
91 Ramesh, Shanti, Morris, & Durairaj, 2011; Ramesh, Shanti, & Morris, 2012; Wang,
92 Zhang, Liu, & He, 2009a; Wang, Zhang, Wang, & Liu, 2009b; Wang, Zhang, Liu, &
93 Han, 2010b). Nevertheless, work reported to date mostly involved processing in solution,
94 whereas melt processing should be more relevant to industry application as much less
95 solvent is required and higher efficiency is expected. Sankri et al. (2010) and Leroy,
96 Jacquet, Coativy, Reguerre, and Lourdin (2012) have done pioneering work using an IL
97 (1-butyl-3-methylimidazolium chloride, or [Bmim][Cl]) as a new plasticiser for melt
98 processing of starch-based materials, which demonstrated improved plasticisation,
99 electrical conductivity, and hydrophobicity. Our previous work (Xie et al., 2014) has
100 shown that an IL, 1-ethyl-3-methylimidazolium acetate ([Emim][OAc]), has a significant
101 plasticisation effect including for a high-amylose starch, prepared via a simple
102 compression moulding process; and can reduce the crystallinity and make the amorphous
103 phase more mobile, advantageous for some specific applications (e.g. electrically
104 conductive materials).

105 This paper reports studies aimed at understanding the plasticisation effect of starch by
106 ILs. Based on the established protocol (Xie et al., 2014), we investigate how the amylose
107 content of starch can influence the characteristics of starch-based materials plasticised by
108 the IL, [Emim][OAc]. It is well established that the amylose content can greatly

109 influence starch granule architecture and molecular structure (Blazek et al., 2009;
110 Cheetham & Tao, 1997; Jenkins & Donald, 1995; Shi, Capitani, Trzasko, & Jeffcoat,
111 1998), thermal behaviour (Liu, Yu, Xie, & Chen, 2006; Liu et al., 2011), processing and
112 rheological behaviour (Chaudhary, Miler, Torley, Sopade, & Halley, 2008; Chinnaswamy
113 & Hanna, 1988; Della Valle, Colonna, Patria, & Vergnes, 1996; Li et al., 2011; Wang et
114 al., 2010a; Xie et al., 2009), and the structure and properties of resulting starch-based
115 materials (Chaudhary, Torley, Halley, McCaffery, & Chaudhary, 2009; Cheetham & Tao,
116 1998; Forssell, Lahtinen, Lahelin, & Myllärinen, 2002; Li et al., 2011; Lourdin, Della
117 Valle, & Colonna, 1995; Mondragón, Mancilla, & Rodríguez-González, 2008; Rindlav-
118 Westling, Stading, & Gatenholm, 2001; Rindlav-Westling, Stading, Hermansson, &
119 Gatenholm, 1998; van Soest & Borger, 1997). In order to reveal the effect of amylose
120 content in the current study, a simple one-step compression moulding process was
121 employed to minimise the effect of shear-induced macromolecular degradation during
122 processing. Moreover, considering that starch is a hydrophilic biopolymer sensitive to
123 environmental moisture and that [Emim][OAc], an hydrophilic IL, may have some
124 impact on the hydrophilicity of starch-based materials, the effect of relative humidity
125 (RH) during ageing of the materials on the material characteristics was also investigated.
126 Thus, the plasticisation effects of [Emim][OAc] on the crystalline structure, mechanical
127 properties, glass transition temperature, thermal stability, and electrical conductivity of
128 the starch-based films are reported here, with the aim of providing information for
129 designing starch plasticisation processes and starch-based materials with tailored
130 properties.
131

132 **2. Materials and Methods**

133 *2.1. Materials*

134 Two commercially available maize starches, Gelose 80 (G80) and regular maize
135 starch (RMS) were used in this work. RMS was supplied by New Zealand Starch Ltd.
136 (Onehunga, Auckland, New Zealand) with the product name Avon Maize Starch; and
137 G80 was supplied by Ingredion ANZ Pty Ltd (Lane Cove, NSW, Australia). Both
138 starches were chemically unmodified and their amylose contents were 24.4% and 82.9%,
139 respectively, as measured previously (Tan, Flanagan, Halley, Whittaker, & Gidley, 2007).
140 The original moisture content of the two starches were 14.1 wt.% and 14.4 wt.%
141 respectively, as measured by a Satorius Moisture Analyser (Model MA30, Sartorius
142 Weighing Technology GmbH, Weender Landstraße 94–108, 37075, Goettingen,
143 Germany). Deionised water was used in all instances. Glycerol (AR) was supplied by
144 Chem-Supply Pty Ltd (Gillman, SA, Australia) and used as received. [Emim][OAc] of
145 purity $\geq 95\%$, produced by IoLiTec Ionic Liquids Technologies GmbH (Salzstraße 184,
146 D-74076 Heilbronn, Germany), was also supplied by Chem-Supply Pty Ltd.
147 [Emim][OAc] was used as received without further purification. As [Emim][OAc] was
148 liquid at room temperature miscible with water (Mateyawa et al., 2013), different ratios
149 of water–[Emim][OAc] mixture could be easily prepared in vials for subsequent use.

150

151 *2.2. Sample preparation*

152 Formulations for sample preparation are shown in Table 1. In Table 1 and the
153 following text, the plasticised starch samples are coded in the format of “G80-18-L”,
154 where “G80” denotes the type of starch, “18” indicates the weight content of the ionic

155 liquid, and “L” means the RH during conditioning (either L, low, 33%; M, medium, 52%;
156 or H, high, 75%). Based on our preliminary work (Xie et al., 2014), the added water–
157 [Emim][OAc] mixture content was fixed at 30% by weight on the basis of the starch wet
158 weight. The liquid mixture was added drop-wise to the starch, accompanied by careful
159 blending using a mortar and pestle to ensure an even distribution of the liquid mixture in
160 the starch. Then, the blended samples were hermetically stored in ziplock bags at 4 °C
161 for at least overnight, before thermal compression moulding. This allowed time for
162 further equilibration of the samples. The powder was carefully and equally spread over
163 the moulding area with poly(tetrafluoroethylene) glass fabrics (Dotmar EPP Pty Ltd,
164 Acacia Ridge, Qld, Australia) located between the starch and the mould, then
165 compression moulded at 160 °C and 6 MPa for 10 min, followed by rapidly cooling to
166 room temperature (RT) before opening the mould and retrieving the sample (thickness
167 approx. 1.2 mm). The films were conditioned at different RHs, 33% (over saturated
168 magnesium chloride solution), 52% (over saturated magnesium nitrate solution), and 75%
169 (over saturated sodium chloride solution), at RT in desiccators for one month before any
170 characterisation of the materials. After the conditioning, the thickness of the films was
171 about 1 mm. The final water contents in the conditioned samples were calculated based
172 on the weight data before and after vacuum-oven drying at 100 °C for two days.

173

174

175 [Insert Table 1 here]

176

177

178 According to our preliminary work (Xie et al., 2014), the use of compression
179 moulding under the described conditions should mostly destroy the starch granules so
180 that plasticised starch could be formed.

181

182 2.3. Characterisation

183 2.3.1. X-ray diffraction (XRD)

184 The starch samples were placed in the sample holder of a powder X-ray
185 diffractometer (D8 Advance, Bruker AXS Inc., Madison, WI, USA) equipped with a
186 graphite monochromator, a copper target, and a scintillation counter detector. XRD
187 patterns were recorded for an angular range (2θ) of 4–40°, with a step size of 0.02° and a
188 step rate of 0.5 s per step, and thus the scan time lasted for approximately 15 min. The
189 radiation parameters were set as 40 kV and 30 mA, with a slit of 2 mm. Traces were
190 processed using the Diffracplus Evaluation Package (Version 11.0, Bruker AXS Inc.,
191 Madison, WI, USA) to determine the X-ray diffractograms of the samples. The degree of
192 crystallinity was calculated using the method of Lopez-Rubio, Flanagan, Gilbert, and
193 Gidley (2008) with the PeakFit software (Version 4.12, Systat Software, Inc., San Jose,
194 CA, USA), Eq. (1):

195

$$196 \quad X_c = \frac{\sum_{i=1}^n A_{ci}}{A_t} \quad (1)$$

197

198 where A_{ci} is the area under each crystalline peak with index i , and A_t is the total area (both
199 amorphous background and crystalline peaks) under the diffractogram.

200 The V-type crystallinity (single-helical amylose structure) was calculated based on
201 the total crystalline peak areas at 7.5, 13, 20, and 23° (van Soest, Hullemann, de Wit, &
202 Vliegthart, 1996).

203

204 2.3.2. NMR

205 The rigid components (short-range orders and rigid amorphous starch) of the starch-
206 based films were examined by solid-state ¹³C cross-polarization magic angle spinning
207 nuclear magnetic resonance (¹³C CP/MAS NMR) experiments at a ¹³C frequency of
208 75.46 MHz on a Bruker MSL-300 spectrometer. Using scissors, the sheets were cut into
209 small evenly sized pieces and were packed in a 4-mm diameter, cylindrical, PSZ
210 (partially-stabilized zirconium oxide) rotor with a KelF end cap. The rotor was spun at
211 5 kHz at the magic angle (54.7°). The 90° pulse width was 5 μs and a contact time of
212 1 ms was used for all samples with a recycle delay of 3 s. The spectral width was 38 kHz,
213 acquisition time 50 ms, time domain points 2 k, transform size 4 k, and line broadening
214 50 Hz. At least 2400 scans were accumulated for each spectrum. Spectra were
215 referenced to external adamantane and analysed by resolving the spectra into ordered and
216 amorphous sub-spectra and calculating the relative areas as described previously (Tan et
217 al., 2007).

218 The amounts of “mobile amorphous starch” and “rigid amorphous starch” were
219 calculated according to our method reported previously (Xie et al., 2014). Briefly, it was
220 assumed that all the crystalline starch was described by the XRD crystal-defect fitting.
221 Then, the difference in the percentage between amorphous starch calculated from XRD

222 and that from ^{13}C CP/MAS NMR was considered to be due to the mobile amorphous
223 starch.

224

225 2.3.3. *Tensile testing*

226 Tensile tests were performed with an Instron[®] 5543 universal testing machine
227 (Instron Pty Ltd, Bayswater, Vic., Australia) with a 500 N load cell on dumbbell-shaped
228 specimens cut from the sheets with a constant deformation rate of 10 mm/min at room
229 temperature. The specimens corresponded to Type 4 of the Australian Standard AS
230 1683:11 (ISO 37:1994), and the testing section of each specimen was 12 mm in length
231 and 2 mm in width. Young's modulus (E), tensile strength (σ_t), and elongation at break
232 (ε_b) were determined by the Instron[®] computer software, from at least 7 specimens for
233 each of the plasticised starch samples.

234

235 2.3.4. *Dynamic mechanical thermal analysis (DMTA)*

236 Dynamic mechanical thermal analysis (DMTA) was performed on rectangular
237 sections taken from tensile bars of the plasticised starch samples using a Rheometric
238 Scientific[™] DMTA IV machine (Rheometric Scientific, Inc., Piscataway, NJ, USA) in
239 the dual cantilever bending mode from -100 to 110 °C, with a heating rate of 3 K/min, a
240 frequency of 1 Hz, and a strain value of 0.05%. The dynamic storage modulus (E'), loss
241 modulus (E''), and loss tangent ($\tan \delta = E''/E'$) were obtained. To prevent water
242 evaporation during the measurements, the specimens were coated with Vaseline grease.
243 No swelling of the specimens was observed, suggesting no adverse effect of the Vaseline.

244

245 2.3.5. *Thermogravimetric analysis (TGA)*

246 A Mettler Toledo TGA/DSC1 machine (Mettler-Toledo Ltd., Port Melbourne, Vic.,
247 Australia) was used with 40 μ L aluminium crucibles for thermogravimetric analysis
248 (TGA) under nitrogen. A sample mass of about 5 mg was used for each run. The
249 samples were heated from 25 $^{\circ}$ C to 550 $^{\circ}$ C at 3 K/min.

250

251 2.3.6. *Electrical conductivity*

252 Volume resistivity measurements were performed on the different starch-based films.
253 The resistivity of samples (circular with diameter of 60 mm) was measured in triplicate
254 using a Keithley electrometer (Model 6517A, Keithley Instruments, Inc., Cleveland, OH,
255 USA) equipped with an 8009 test fixture and employing the Keithley Alt-Polarity method.
256 The sample of interest was placed between two annular electrodes and the volume
257 resistivity measured by applying a DC voltage potential across opposite sides of the
258 sample and measuring the resultant current through the sample. This test conforms to
259 ASTM D-257. The corresponding electrical conductivity values were obtained as the
260 inverse of the volume resistivity values.

261

262 **3. Results and Discussion**

263 3.1. *Moisture contents*

264 While different formulations were used for preparing the samples, the water contents
265 in the final samples could be largely varied by compression moulding and conditioning.
266 Table 1 shows that the final water content was both affected by the original IL content
267 and the RH during conditioning, but not the starch type — generally for both starches a

268 higher IL content and/or a higher RH during conditioning could lead to a higher final
269 water content. It is noteworthy that except G80-27-H and RMS-27-H, the final water
270 contents were lower than the water contents in original formulations, meaning that water
271 desorption occurred during conditioning for most of the samples. This could suggest that
272 there were very strong interactions between the IL and the starch, so both of them had
273 much smaller chance to interact with water. In this case, the free water could mostly
274 evaporate to the environment during the long-time conditioning. Unlike previous studies
275 of solutions of starch, water and [Emim][OAc] (Mateyawa et al., 2013) where
276 preferential interactions between water and the IL were proposed, the current work
277 involves formulations containing starch as the main component for melt processing.
278 Thus, although the water–[Emim][OAc] mixture was initially added into the starch (and
279 strong interactions between [OAc⁻] anions and water could firstly form (Hall et al.,
280 2012)), during conditioning the IL might change to preferably interact with the abundant
281 starch hydroxyls, resulting in its dissociation with water. Previous studies have suggested
282 that IL anions could act as proton acceptors to form hydrogen bonding with the
283 biopolymer hydroxyls (Abe, Fukaya, & Ohno, 2012; Fukaya, Sugimoto, & Ohno, 2006;
284 Remsing, Swatloski, Rogers, & Moyna, 2006; Zhang et al., 2014). Nonetheless, the
285 mechanism for the change of interactions shown in the current work is worth further
286 investigation.

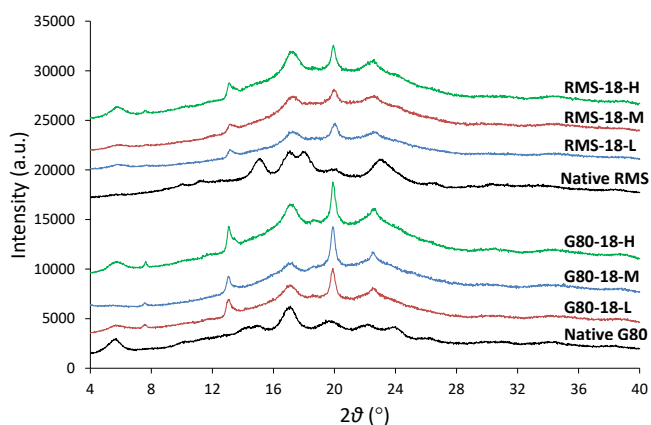
287

288 3.2. *Structural characteristics*

289 Figure 1 shows the XRD patterns of the two native starches and their plasticised
290 samples. Native G80 showed a strong diffraction peak at a 2θ position of around 17° ,

291 with a few smaller peaks at 2θ of approximately 5° , 10° , 14° , 15° , 19° , 22° , 23° , 26° , 31° ,
 292 and 34° , indicative of B-type crystalline structure (Cheetham & Tao, 1998; Tan et al.,
 293 2007). After processing, besides the original B-type characteristic peaks (main peak at
 294 $2\theta \approx 17^\circ$), all the starch samples displayed peaks at 2θ of around 7° , 13° , 20° , and 22° ,
 295 characteristic of V_H -type crystalline structure, a single-helical amylose structure (similar
 296 to that formed by amylose–lipid helical complexes) and is well known for thermally-
 297 processed (e.g., compression moulding and extrusion) starch-based materials (van Soest
 298 et al., 1996). That is, the plasticised samples contained crystalline structure not
 299 destructured by compression moulding (which is normal in starch processing) and some
 300 newly formed V_H -type crystalline structure mainly induced by processing (and possibly
 301 also some newly formed B-type crystalline structure during ageing with moisture) (van
 302 Soest et al., 1996; van Soest & Borger, 1997).

303



304

305 Figure 1 XRD results of G80 and RMS native starches and the different starch-based
 306 films. “L”, “M”, and “H” (shown by different colours) correspond to samples
 307 after conditioning at low (33%), medium (52%) and high (75%) relative
 308 humidity.

309

310

311 On the other hand, it can be seen from Figure 1 that native RMS showed typical A-
312 type pattern, with strong reflections at 2θ of about 15° and 23° and an unresolved doublet
313 at 2θ of 17° and 18° , with a few weak peaks at 2θ of about 26° , 30° , and 33° (Cheetham
314 & Tao, 1998; Tan et al., 2007). For the plasticised samples, the doublet at 2θ of 17° and
315 18° disappeared, suggesting a complete loss of A-type pattern. Besides, the plasticised
316 samples displayed strong V_H -type pattern as shown by sharp peaks at 2θ of 7° , 13° , 20° ,
317 and 22° (van Soest et al., 1996), and B-type pattern as indicated by strong reflections at
318 2θ of 5° and 17° (Cheetham & Tao, 1998; Tan et al., 2007). As for the plasticised G80
319 samples, the plasticised RMS has both (newly formed) V_H -type and B-type crystalline
320 structures.

321 Table 2 shows the contents of double-helices (A- or B-type crystalline structure),
322 single-helices (V-type crystalline structure), and amorphous parts of the plasticised starch
323 samples as measured by XRD and NMR. Native G80 has a degree of crystallinity of
324 32.2%, and this value was greatly reduced in the processed and plasticised samples.
325 Native RMS has a higher degree of crystallinity, 39.5%, which also decreased
326 significantly after processing. The plasticised G80 samples overall had a higher degree
327 of total crystallinity compared with the RMS samples. This could be because of the
328 higher amount of double-helices remaining (and/or formed during processing), and the
329 higher content of V-type crystalline structure formed in the plasticised G80 samples.
330 However, for both starches no apparent difference in total crystallinity could be seen as a
331 result of the different conditioning RHs, although the diffraction peaks were sharper after

332 higher RH conditioning, showing that crystallites within the sample were either larger or
333 more perfect. It could be possible that the IL, which was more effective in the interaction
334 with starch, governed the disruption of original crystalline structure as well as the
335 formation of new crystalline structure, making the effect of environmental RH, and thus
336 the sample water content, much less important. Moreover, it can be seen from Table 2
337 that the G80-based films had a higher mobile amorphous component (%) than that of the
338 RMS films. As the sample water content was not apparently affected by the starch type,
339 the differences in mobile amorphous component could be associated with the higher
340 amylose content in G80. When plasticised by the IL, the linear amylose molecules could
341 be more mobile than the highly short-branched amylopectin molecules. The more rigid
342 molecular structure of amylopectin has already been proposed elsewhere (Liu, Halley, &
343 Gilbert, 2010; Xie et al., 2009).

344

345

346 [Insert Table 2 here]

347

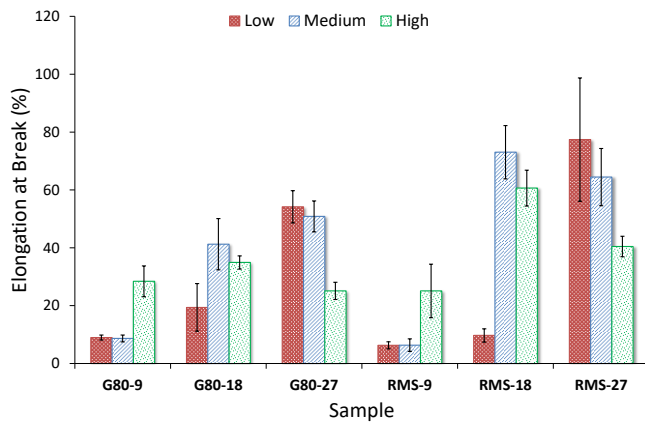
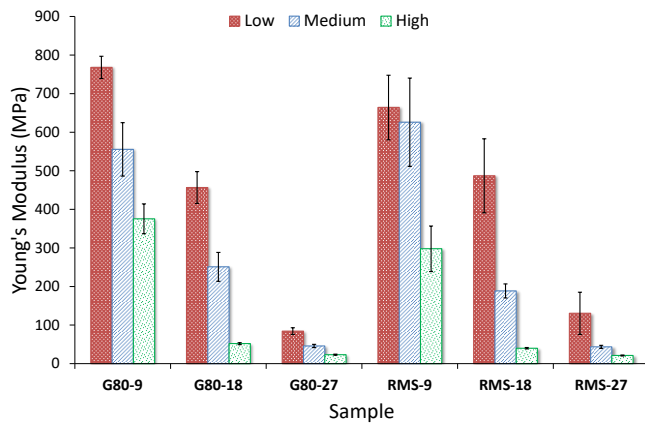
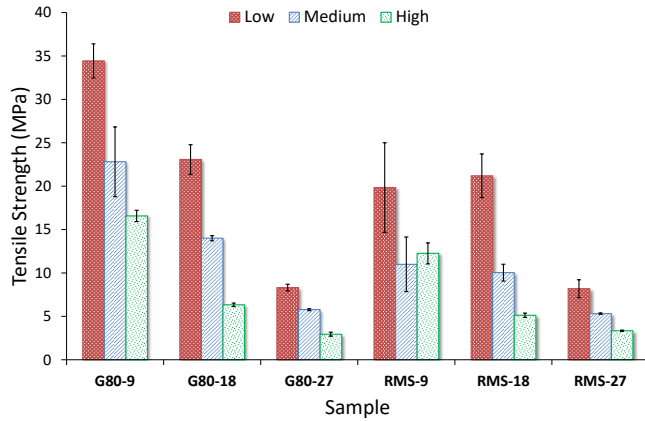
348

349 3.3. *Mechanical properties*

350 Figure 2 shows the tensile mechanical properties of the different starch samples. A
351 higher content of [Emim][OAc] contributed to lower σ_t and E , as reported previously
352 (Xie et al., 2014). In addition, σ_t and E also decreased as the RH (and thus the sample
353 water content) increased. Since XRD and NMR results have already shown the
354 insignificance of RH on starch molecular and crystalline orders and that crystallinity was

355 mostly low, the trend observed here is most likely due to the plasticisation effect of
356 [Emim][OAc] and water (although [Emim][OAc] might be more important based on the
357 discussion on moisture contents). Both the IL and water could disrupt hydrogen bonding
358 between starch molecules, and form hydrogen bonding with the –OH sites of starch,
359 resulting in reduced strength and stiffness. Additionally, there was little apparent effect
360 of amylose content on σ_t or E (noting that with certain formulations and conditioning
361 RHs, the final water contents were quite similar in different amylose-content samples)
362 except that G80-9 had higher σ_t values than those of RMS-9. It is proposed that when the
363 material is well plasticised, the macromolecular structure (amylose or amylopectin) plays
364 a minor role in determining mechanical properties. That is, the entanglement of
365 macromolecules (mainly amylose) is not a major influence on mechanical properties.

366



367

368 Figure 2 Tensile strength (σ_t) (upper), Young's modulus (E) (middle), and elongation at
 369 break (ϵ_b) (lower) of the different starch-based films. The error bars represent
 370 standard deviations. "Low", "Medium", and "High" (shown by different
 371 colours and patterns) correspond to samples after conditioning at low (33%),
 372 medium (52%) and high (75%) relative humidity.

373

374

375 The ε_b value was also affected by the RH (and thus the sample water content), but in a
376 more complex way. It was observed from Figure 2 that increase in RH could either
377 increase or decrease ε_b , depending on [Emim][OAc] content. When the [Emim][OAc]
378 content was 18 wt.%, increase in RH initially increased ε_b remarkably and then decreased
379 this value to some extent. Nevertheless, when the [Emim][OAc] content was 27%,
380 increase in RH from 33% to 75% decreased ε_b progressively. It is proposed that the IL
381 could disrupt starch H-bonding and prevent macromolecular entanglement, making the
382 polymer have less “connections” between its chains and become “weaker”. And also
383 when the material was “softened” too much by plasticisation, there was no work
384 hardening to stabilise drawing, as indicated by increased ε_b . In addition, it can be noticed
385 that when the material was well plasticised but not “too soft” (the [Emim][OAc] content
386 18%), RMS could lead to a higher value of ε_b than that for G80. This differs from the
387 results of extruded starch-based films that show higher ε_b in starch with a higher amylose
388 content (Li et al., 2011). Here with, again, much less entanglement of macromolecules
389 (mainly amylose) due to the plasticisation by [Emim][OAc], the major reason accounting
390 for the moderately higher ε_b for the RMS samples might be the much bigger size of
391 amylopectin macromolecules which could be stretched more before breaking.

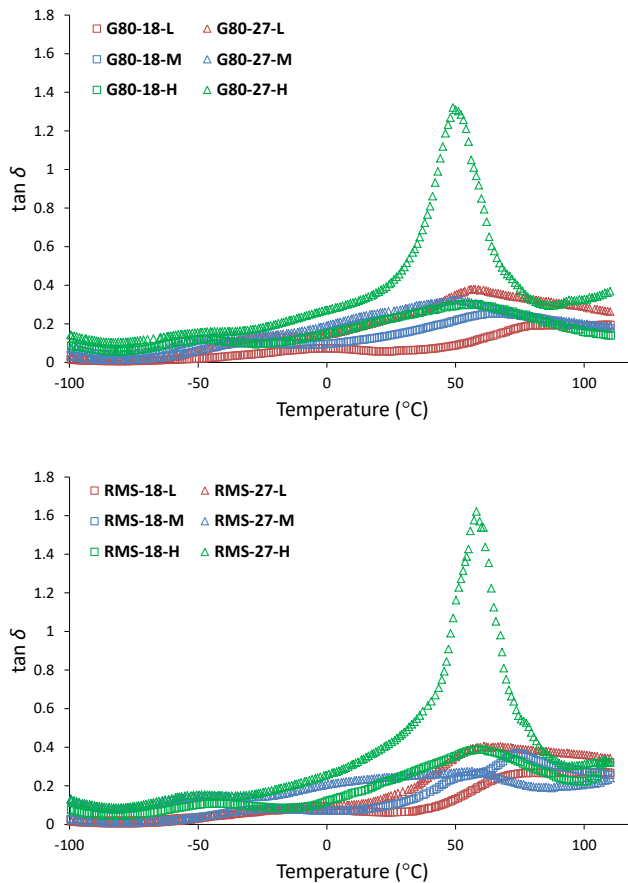
392

393 3.4. DMTA analysis

394 Figure 3 shows the DMTA results of the different starch samples. For some of the
395 samples, a prominent peak was shown between 30 °C and 100 °C. Based on previous

396 studies (Madrigal, Sandoval, & Müller, 2011; Perdomo et al., 2009), this peak can be
397 attributed to the glass transition of starch (T_g), which will be the main focus of the
398 discussion below. Prior to this peak, another moderate peak can be seen at a lower
399 temperature (between -80 °C and 30 °C depending on sample) which can be ascribed to
400 the glass transition of plasticiser-rich domains.

401



402

403 Figure 3 $\tan \delta$ of the different starch-based films (top: G80; bottom: RMS). “L”, “M”,
404 and “H” (shown by different colours) correspond to samples after conditioning
405 at low (33%), medium (52%) and high (75%) relative humidity.

406

407

408 It can be seen from Figure 3 that, for both G80 and RMS, the samples with 27 wt.%
409 [Emim][OAc] content normally had lower T_g than those with 18 wt.% [Emim][OAc], but
410 a more intense peak height. This could be attributed to the greater plasticisation effect of
411 [Emim][OAc] relative to that of water (Xie et al., 2014). For the samples conditioned at
412 low and medium RH, there was a big difference in how the T_g varied with [Emim][OAc]
413 content (cf. Table 3). For example, for the plasticised G80 samples conditioned at low
414 RH, T_g with 18 wt.% [Emim][OAc] content was 79 °C, which decreased to 57 °C when
415 the [Emim][OAc] content was increased to 27 wt.%. For the RMS samples conditioned
416 at low RH, T_g was 76 °C with 18 wt.% [Emim][OAc] content, while T_g was 61 °C with
417 27 wt.% [Emim][OAc] content. For both starch samples conditioned at high RH, when
418 the [Emim][OAc] content was 18 wt.%, the peak height was still at a level comparable to
419 those in the cases discussed above; however, when the [Emim][OAc] content was
420 changed to 27 wt.%, a strong and sharp peak representing the glass transition of starch
421 was observed. This apparent transition could be associated with the greater mobility
422 assisted by the highest contents of both [Emim][OAc] and water (resulting from high
423 RH). Nonetheless, for the samples conditioned at high RH (thus with the highest water
424 contents), when the [Emim][OAc] content was changed from 18 wt.% to 27 wt.%, T_g did
425 not vary much, from 52 °C to 49 °C for G80 and from 59 °C to 58 °C for RMS. It is
426 proposed that once the starch macromolecules are saturated with plasticisers, further
427 addition of plasticiser will not change the molecular mobility (reflected by T_g) any further.
428
429
430 [Insert Table 3 here]

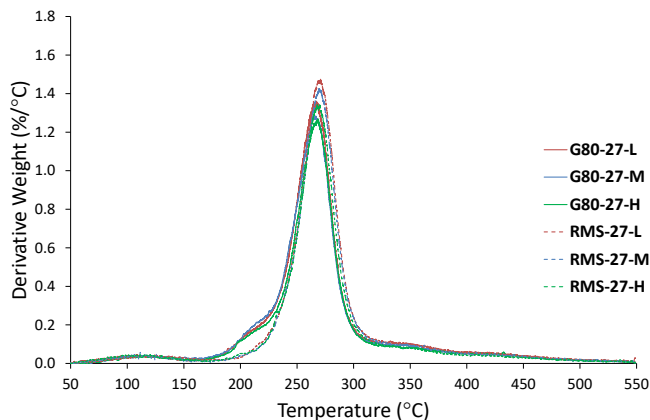
431

432

433 3.5. TGA

434 Our previous report has shown that [Emim][OAc] has an obvious effect in reducing
435 the thermal decomposition temperature of starch-based materials (Xie et al., 2014). The
436 effects of conditioning RH and amylose content were further investigated here and the
437 results are shown in Figure 4. It can be seen that all samples had a major derivative
438 weight percentage peak between 200 °C and 350 °C, after a gentle hump ranging from
439 50 °C to 170 °C. The large peak can be associated with the breakage of long chains of
440 starch as well as the destruction (oxidation) of the glucose rings (Liu, Yu, Liu, Chen, &
441 Li, 2009b), while the smaller hump can be ascribed to moisture loss from the samples.
442 For the RMS samples, there seemed to be a small shoulder peak between 190 °C and
443 230 °C, which overlapped with the major peak. This peak can be specifically ascribed to
444 the breakage of starch long chains (Liu et al., 2009b). With a lower amylose/amylopectin
445 ratio (increased molecular weight), this peak moves to a higher temperature, thus merging
446 into the major peak (Liu et al., 2009b). Therefore, for RMS, this small peak could not be
447 seen. Besides this small peak, the results here show no apparent difference in the thermal
448 stability between the samples of different amylose contents as well as those with different
449 water contents (conditioned at different RHs), which is similar to the results for starch
450 with only water (Liu et al., 2009b).

451



452

453 Figure 4 TGA results of the different starch-based films. “L”, “M”, and “H” (shown by
 454 different colours) correspond to samples after conditioning at low (33%),
 455 medium (52%) and high (75%) relative humidity.

456

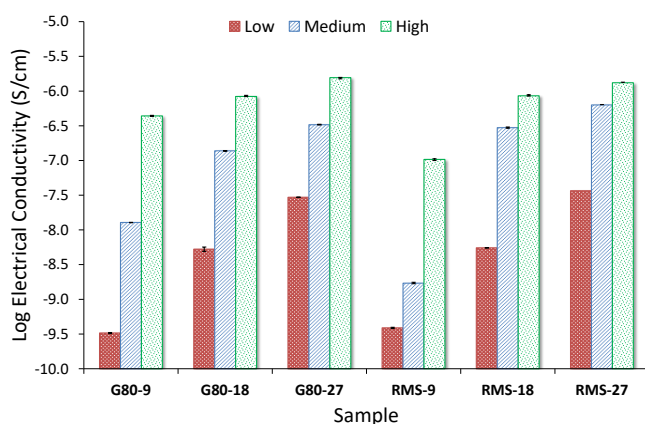
457

458 3.6. *Electrical conductivity*

459 The electrical conductivity results for the different samples are shown in Figure 5. It
 460 can be seen that the electrical conductivity ranged between $10^{-9.5}$ to $10^{-5.8}$ S/cm for
 461 different formulations. Wang et al. (2009a) prepared starch-based films plasticised by
 462 30 wt.% 1-allyl-3-methylimidazolium chloride ([Amim][Cl]), which had electrical
 463 conductivity as high as $10^{-1.6}$ S/cm at 14.5 wt.% water content. Sankri et al. (2010)
 464 showed that starch-based films plasticised by 30 wt.% 1-butyl-3-methylimidazolium
 465 chloride ([Bmim][Cl]) had electrical conductivity of $10^{-4.6}$ S/cm at 13 wt.% water content.
 466 Sankri et al. (2010) further proposed that the high electrical conductivity obtained by
 467 Wang et al. (2009a) may be explained by increased ion mobility due to the ion pair
 468 dissociation mechanism described by Zhang et al. (2005), and this ion pair dissociation
 469 might not be apparent for [Amim][Cl] resulting in more localised ions in the case of

470 [Amim][Cl]–plasticised starch. Also, as the conductivity is mainly controlled by ion
 471 diffusivity and mobility, the anion should be small, with delocalized charge. For the
 472 lower electrical conductivity of [Emim][OAc]–plasticised starch in this study as
 473 compared to those of starch-based materials plasticised by other ILs in the literature, the
 474 lower extent of ion pair dissociation and the anion size might be a reason, while the
 475 smaller amount ($\leq 27\%$) of IL in starch should also be considered.

476



477

478 Figure 5 Electrical conductivity of the different starch-based films. The error bars
 479 represent standard deviations. “Low”, “Medium”, and “High” (shown by
 480 different colours and patterns) correspond to samples after conditioning at low
 481 (33%), medium (52%) and high (75%) relative humidity.

482

483

484 From Figure 5, a general trend could be identified in that both increase in RH and
 485 [Emim][OAc] content could increase the electrical conductivity, with the effect of RH
 486 being more significant. Wang et al. (2009a) have indicated that increasing ion
 487 concentration by increasing the IL content could improve the conductance of plasticised

488 starch films effectively, and high water content can be advantageous to the transference
489 of the anions and cations in plasticised starch films. Nevertheless, there was no apparent
490 trend regarding the influence of amylose content on electrical conductivity. The
491 plasticised G80 samples with 9% [Emim][OAc] content conditioned at the medium and
492 high RH seemed to have higher electrical conductivity than the plasticised RMS samples
493 with the same [Emim][OAc] content conditioned at the same RHs. But this may need
494 further investigation.

495

496 **4. Conclusion**

497 It is well established in the literature that the amylose content of starch can greatly
498 influence the structure and properties of starch-based materials. However, this study
499 showed that the amylose content could only have some degree of influence on the
500 crystalline structure and the mobility of the amorphous chain segments in [Emim][OAc]-
501 plasticised starch. Nevertheless, this structural difference was shown to not significantly
502 impact on mechanical properties, glass transition temperature, thermal stability, nor
503 electrical conductivity of plasticised starch films. This may be ascribed in part to the
504 relatively low degree of crystallinity in the starch samples, meaning that the plasticisation
505 of starch macromolecules by [Emim][OAc] and water could play a major role in
506 determining material characteristics. Furthermore, the strong plasticisation effect
507 imparted by [Emim][OAc] compared to other plasticisers could make entanglement of
508 starch macromolecules (mainly amylose) much less significant. As a result, rather than
509 the IL content, RH conditioning and thus the sample water content predominantly

510 influenced mechanical properties, glass transition temperature, and electrical
511 conductivity.

512 Overall, this study suggests that, with the strong plasticisation effect of an IL, the
513 effect of amylose content on characteristics of starch-based materials could become
514 unimportant, thus the use of relatively more expensive high-amylose starches can be
515 unnecessary for the formation of mechanically-useful structures in biomaterials
516 applications. This study also shows the potential of IL-plasticised starch-based materials
517 in applications as smart devices where the control of material characteristics by
518 environmental RH is desirable.

519

520 **Acknowledgements**

521 The research leading to these results has received funding from the Australian
522 Research Council (ARC) under the Discovery Project No. 120100344. M. Li also would
523 like to thank the China Scholarship Council (CSC) for providing research funding for her
524 Ph.D. study at The University of Queensland (UQ). The authors acknowledge the
525 facilities, and the scientific and technical assistance, of the Australian Microscopy &
526 Microanalysis Research Facility (AMMRF) at the Centre for Microscopy and
527 Microanalysis (CMM), UQ.

528

529 **References**

530 Abe, M., Fukaya, Y., & Ohno, H. (2012). Fast and facile dissolution of cellulose with
531 tetrabutylphosphonium hydroxide containing 40 wt% water. *Chemical*
532 *Communications*, 48(12), 1808-1810.

533 Avérous, L. (2004). Biodegradable multiphase systems based on plasticized starch: a
534 review. *Polymer Reviews*, 44(3), 231-274.

535 Biswas, A., Shogren, R. L., Stevenson, D. G., Willett, J. L., & Bhowmik, P. K. (2006).
536 Ionic liquids as solvents for biopolymers: Acylation of starch and zein protein.
537 *Carbohydrate Polymers*, 66(4), 546-550.

538 Blazek, J., Salman, H., Rubio, A. L., Gilbert, E., Hanley, T., & Copeland, L. (2009).
539 Structural characterization of wheat starch granules differing in amylose content and
540 functional characteristics. *Carbohydrate Polymers*, 75(4), 705-711.

541 Chaudhary, A. L., Miler, M., Torley, P. J., Sopade, P. A., & Halley, P. J. (2008).
542 Amylose content and chemical modification effects on the extrusion of thermoplastic
543 starch from maize. *Carbohydrate Polymers*, 74(4), 907-913.

544 Chaudhary, A. L., Torley, P. J., Halley, P. J., McCaffery, N., & Chaudhary, D. S. (2009).
545 Amylose content and chemical modification effects on thermoplastic starch from
546 maize - Processing and characterisation using conventional polymer equipment.
547 *Carbohydrate Polymers*, 78(4), 917-925.

548 Cheetham, N. W. H., & Tao, L. (1997). The effects of amylose content on the molecular
549 size of amylose, and on the distribution of amylopectin chain length in maize
550 starches. *Carbohydrate Polymers*, 33(4), 251-261.

551 Cheetham, N. W. H., & Tao, L. (1998). Variation in crystalline type with amylose
552 content in maize starch granules: an X-ray powder diffraction study. *Carbohydrate
553 Polymers*, 36(4), 277-284.

554 Chinnaswamy, R., & Hanna, M. A. (1988). Relationship between amylose content and
555 extrusion-expansion properties of corn starches. *Cereal Chemistry*, 65(2), 138-143.

556 Della Valle, G., Colonna, P., Patria, A., & Vergnes, B. (1996). Influence of amylose
557 content on the viscous behavior of low hydrated molten starches. *Journal of*
558 *Rheology*, 40(3), 347-362.

559 El Seoud, O. A., Koschella, A., Fidale, L. C., Dorn, S., & Heinze, T. (2007). Applications
560 of ionic liquids in carbohydrate chemistry: A window of opportunities.
561 *Biomacromolecules*, 8(9), 2629-2647.

562 Forssell, P., Lahtinen, R., Lahelin, M., & Myllärinen, P. (2002). Oxygen permeability of
563 amylose and amylopectin films. *Carbohydrate Polymers*, 47(2), 125-129.

564 Fu, Z.-q., Wang, L.-j., Li, D., Wei, Q., & Adhikari, B. (2011). Effects of high-pressure
565 homogenization on the properties of starch-plasticizer dispersions and their films.
566 *Carbohydrate Polymers*, 86(1), 202-207.

567 Fukaya, Y., Sugimoto, A., & Ohno, H. (2006). Superior solubility of polysaccharides in
568 low viscosity, polar, and halogen-free 1, 3-dialkylimidazolium formates.
569 *Biomacromolecules*, 7(12), 3295-3297.

570 Hall, C. A., Le, K. A., Rudaz, C., Radhi, A., Lovell, C. S., Damion, R. A., et al. (2012).
571 Macroscopic and microscopic study of 1-ethyl-3-methyl-imidazolium acetate–water
572 mixtures. *The Journal of Physical Chemistry B*, 116(42), 12810-12818.

573 Heinze, T., Schwikal, K., & Barthel, S. (2005). Ionic liquids as reaction medium in
574 cellulose functionalization. *Macromolecular Bioscience*, 5(6), 520-525.

575 Jane, J.-I. (2009). Structural features of starch granules II. In B. James, & W. Roy (Eds.),
576 *Starch (Third Edition)* (pp. 193-236). San Diego: Academic Press.

577 Jenkins, P. J., & Donald, A. M. (1995). The influence of amylose on starch granule
578 structure. *International Journal of Biological Macromolecules*, 17(6), 315-321.

579 Leroy, E., Jacquet, P., Coativy, G., Reguerre, A. I., & Lourdin, D. (2012).
580 Compatibilization of starch–zein melt processed blends by an ionic liquid used as
581 plasticizer. *Carbohydrate Polymers*, 89(3), 955-963.

582 Li, M., Liu, P., Zou, W., Yu, L., Xie, F., Pu, H., et al. (2011). Extrusion processing and
583 characterization of edible starch films with different amylose contents. *Journal of*
584 *Food Engineering*, 106(1), 95-101.

585 Liew, C.-W., Ramesh, S., Ramesh, K., & Arof, A. (2012). Preparation and
586 characterization of lithium ion conducting ionic liquid-based biodegradable corn
587 starch polymer electrolytes. *Journal of Solid State Electrochemistry*, 16(5), 1869-
588 1875.

589 Liu, H., Yu, L., Xie, F., & Chen, L. (2006). Gelatinization of cornstarch with different
590 amylose/amylopectin content. *Carbohydrate Polymers*, 65(3), 357-363.

591 Liu, H., Xie, F., Yu, L., Chen, L., & Li, L. (2009a). Thermal processing of starch-based
592 polymers. *Progress in Polymer Science*, 34(12), 1348-1368.

593 Liu, P., Xie, F., Li, M., Liu, X., Yu, L., Halley, P. J., et al. (2011). Phase transitions of
594 maize starches with different amylose contents in glycerol-water systems.
595 *Carbohydrate Polymers*, 85(1), 180-187.

596 Liu, W.-C., Halley, P. J., & Gilbert, R. G. (2010). Mechanism of degradation of starch, a
597 highly branched polymer, during extrusion. *Macromolecules*, 43(6), 2855-2864.

598 Liu, X., Yu, L., Liu, H., Chen, L., & Li, L. (2009b). Thermal decomposition of corn
599 starch with different amylose/amylopectin ratios in open and sealed systems. *Cereal*
600 *Chemistry*, 86(4), 383-385.

601 Lopez-Rubio, A., Flanagan, B. M., Gilbert, E. P., & Gidley, M. J. (2008). A novel
602 approach for calculating starch crystallinity and its correlation with double helix
603 content: A combined XRD and NMR study. *Biopolymers*, 89(9), 761-768.

604 Lourdin, D., Della Valle, G., & Colonna, P. (1995). Influence of amylose content on
605 starch films and foams. *Carbohydrate Polymers*, 27(4), 261-270.

606 Lu, J., Yan, F., & Texter, J. (2009). Advanced applications of ionic liquids in polymer
607 science. *Progress in Polymer Science*, 34(5), 431-448.

608 Madrigal, L., Sandoval, A. J., & Müller, A. J. (2011). Effects of corn oil on glass
609 transition temperatures of cassava starch. *Carbohydrate Polymers*, 85(4), 875-884.

610 Mateyawa, S., Xie, D. F., Truss, R. W., Halley, P. J., Nicholson, T. M., Shamshina, J. L.,
611 et al. (2013). Effect of the ionic liquid 1-ethyl-3-methylimidazolium acetate on the
612 phase transition of starch: Dissolution or gelatinization? *Carbohydrate Polymers*,
613 94(1), 520-530.

614 Mondragón, M., Mancilla, J. E., & Rodríguez-González, F. J. (2008). Nanocomposites
615 from plasticized high-amylopectin, normal and high-amylose maize starches. *Polymer*
616 *Engineering & Science*, 48(7), 1261-1267.

617 Perdomo, J., Cova, A., Sandoval, A. J., García, L., Laredo, E., & Müller, A. J. (2009).
618 Glass transition temperatures and water sorption isotherms of cassava starch.
619 *Carbohydrate Polymers*, 76(2), 305-313.

620 Pérez, S., Baldwin, P. M., & Gallant, D. J. (2009). Structural features of starch granules I.
621 In B. James, & W. Roy (Eds.), *Starch (Third Edition)* (pp. 149-192). San Diego:
622 Academic Press.

623 Pérez, S., & Bertoft, E. (2010). The molecular structures of starch components and their
624 contribution to the architecture of starch granules: a comprehensive review.
625 *Starch/Stärke*, 62(8), 389-420.

626 Phillips, D. M., Drummy, L. F., Conrady, D. G., Fox, D. M., Naik, R. R., Stone, M. O., et
627 al. (2004). Dissolution and regeneration of bombyx mori silk fibroin using ionic
628 liquids. *Journal of the American Chemical Society*, 126(44), 14350-14351.

629 Pu, Y., Jiang, N., & Ragauskas, A. J. (2007). Ionic Liquid as a Green Solvent for Lignin.
630 *Journal of Wood Chemistry and Technology*, 27(1), 23-33.

631 Ramesh, S., Liew, C.-W., & Arof, A. K. (2011). Ion conducting corn starch biopolymer
632 electrolytes doped with ionic liquid 1-butyl-3-methylimidazolium
633 hexafluorophosphate. *Journal of Non-Crystalline Solids*, 357(21), 3654-3660.

634 Ramesh, S., Shanti, R., Morris, E., & Durairaj, R. (2011). Utilisation of corn starch in
635 production of 'green' polymer electrolytes. *Materials Research Innovations*, 15(1), s8.

636 Ramesh, S., Shanti, R., & Morris, E. (2012). Studies on the thermal behavior of
637 CS:LiTFSI:[Amim] Cl polymer electrolytes exerted by different [Amim] Cl content.
638 *Solid State Sciences*, 14(1), 182-186.

639 Remsing, R. C., Swatloski, R. P., Rogers, R. D., & Moyna, G. (2006). Mechanism of
640 cellulose dissolution in the ionic liquid 1-n-butyl-3-methylimidazolium chloride: a 13
641 C and 35/37 Cl NMR relaxation study on model systems. *Chemical*
642 *Communications*(12), 1271-1273.

643 Rindlav-Westling, A., Stading, M., & Gatenholm, P. (2001). Crystallinity and
644 morphology in films of starch, amylose and amylopectin blends. *Biomacromolecules*,
645 3(1), 84-91.

646 Rindlav-Westling, Å., Stading, M., Hermansson, A.-M., & Gatenholm, P. (1998).
647 Structure, mechanical and barrier properties of amylose and amylopectin films.
648 *Carbohydrate Polymers*, 36(2–3), 217-224.

649 Sankri, A., Arhaliass, A., Dez, I., Gaumont, A. C., Grohens, Y., Lourdin, D., et al.
650 (2010). Thermoplastic starch plasticized by an ionic liquid. *Carbohydrate Polymers*,
651 82(2), 256-263.

652 Shi, Y.-C., Capitani, T., Trzasko, P., & Jeffcoat, R. (1998). Molecular structure of a low-
653 amylopectin starch and other high-amylose maize starches. *Journal of Cereal*
654 *Science*, 27(3), 289-299.

655 Tan, I., Flanagan, B. M., Halley, P. J., Whittaker, A. K., & Gidley, M. J. (2007). A
656 method for estimating the nature and relative proportions of amorphous, single, and
657 double-helical components in starch granules by ¹³C CP/MAS NMR.
658 *Biomacromolecules*, 8(3), 885-891.

659 van Soest, J. J. G., Hulleman, S. H. D., de Wit, D., & Vliegenthart, J. F. G. (1996).
660 Crystallinity in starch bioplastics. *Industrial Crops and Products*, 5(1), 11-22.

661 van Soest, J. J. G., & Borger, D. B. (1997). Structure and properties of compression-
662 molded thermoplastic starch materials from normal and high-amylose maize starches.
663 *Journal of Applied Polymer Science*, 64(4), 631-644.

664 Wang, J., Yu, L., Xie, F., Chen, L., Li, X., & Liu, H. (2010a). Rheological properties and
665 phase transition of cornstarches with different amylose/amylopectin ratios under
666 shear stress. *Starch/Stärke*, 62(12), 667-675.

667 Wang, N., Zhang, X., Liu, H., & He, B. (2009a). 1-Allyl-3-methylimidazolium chloride
668 plasticized-corn starch as solid biopolymer electrolytes. *Carbohydrate Polymers*,
669 76(3), 482-484.

670 Wang, N., Zhang, X., Wang, X., & Liu, H. (2009b). Communications: Ionic liquids
671 modified montmorillonite/thermoplastic starch nanocomposites as ionic conducting
672 biopolymer. *Macromolecular Research*, 17(5), 285-288.

673 Wang, N., Zhang, X., Liu, H., & Han, N. (2010b). Ionically conducting polymers based
674 on ionic liquid-plasticized starch containing lithium chloride. *Polymers & Polymer
675 Composites*, 18(1), 53-58.

676 Wang, Q., Chen, Q., Yang, Y., & Shao, Z. (2012). Effect of various dissolution systems
677 on the molecular weight of regenerated silk fibroin. *Biomacromolecules*, 14(1), 285-
678 289.

679 Wang, Q., Yang, Y., Chen, X., & Shao, Z. (2012). Investigation of rheological properties
680 and conformation of silk fibroin in the solution of AmimCl. *Biomacromolecules*,
681 13(6), 1875-1881.

682 Wilpiszewska, K., & Spychaj, T. (2011). Ionic liquids: Media for starch dissolution,
683 plasticization and modification. *Carbohydrate Polymers*, 86(2), 424-428.

684 Wu, Y., Sasaki, T., Irie, S., & Sakurai, K. (2008). A novel biomass-ionic liquid platform
685 for the utilization of native chitin. *Polymer*, 49(9), 2321-2327.

686 Xie, F., Yu, L., Su, B., Liu, P., Wang, J., Liu, H., et al. (2009). Rheological properties of
687 starches with different amylose/amylopectin ratios. *Journal of Cereal Science*, 49(3),
688 371-377.

689 Xie, F., Halley, P. J., & Avérous, L. (2012). Rheology to understand and optimize
690 processibility, structures and properties of starch polymeric materials. *Progress in*
691 *Polymer Science*, 37(4), 595-623.

692 Xie, F., Pollet, E., Halley, P. J., & Avérous, L. (2013). Starch-based nano-biocomposites.
693 *Progress in Polymer Science*, 38(10-11), 1590-1628.

694 Xie, F., Flanagan, B. M., Li, M., Sangwan, P., Truss, R. W., Halley, P. J., et al. (2014).
695 Characteristics of starch-based films plasticised by glycerol and by the ionic liquid 1-
696 ethyl-3-methylimidazolium acetate: a comparative study. *Carbohydrate Polymers*,
697 111, 841-848.

698 Xie, H., Li, S., & Zhang, S. (2005). Ionic liquids as novel solvents for the dissolution and
699 blending of wool keratin fibers. *Green Chemistry*, 7(8), 606-608.

700 Xie, H., Zhang, S., & Li, S. (2006). Chitin and chitosan dissolved in ionic liquids as
701 reversible sorbents of CO₂. *Green Chemistry*, 8(7), 630-633.

702 Yu, L., Dean, K., & Li, L. (2006). Polymer blends and composites from renewable
703 resources. *Progress in Polymer Science*, 31(6), 576-602.

704 Zakrzewska, M. E., Bogel-Lukasik, E., & Bogel-Lukasik, R. (2010). Solubility of
705 carbohydrates in ionic liquids. *Energy & Fuels*, 24(2), 737-745.

706 Zhang, C., Liu, R., Xiang, J., Kang, H., Liu, Z., & Huang, Y. (2014). Dissolution
707 Mechanism of Cellulose in N, N-Dimethylacetamide/Lithium Chloride: Revisiting
708 through Molecular Interactions. *The Journal of Physical Chemistry B*.

709 Zhang, H., Wu, J., Zhang, J., & He, J. (2005). 1-Allyl-3-methylimidazolium chloride
710 room temperature ionic liquid: A new and powerful nonderivatizing solvent for
711 cellulose. *Macromolecules*, 38(20), 8272-8277.

712 Zhu, S., Wu, Y., Chen, Q., Yu, Z., Wang, C., Jin, S., et al. (2006). Dissolution of
713 cellulose with ionic liquids and its application: a mini-review. *Green Chemistry*, 8(4),
714 325-327.
715

716 **Figure captions**

717 Figure 1 XRD results of G80 and RMS native starches and the different starch-based
718 films. “L”, “M”, and “H” (shown by different colours) correspond to samples
719 after conditioning at low (33%), medium (52%) and high (75%) relative
720 humidity.

721 Figure 2 Tensile strength (σ_t) (upper), Young’s modulus (E) (middle), and elongation at
722 break (ϵ_b) (lower) of the different starch-based films. The error bars represent
723 standard deviations. “Low”, “Medium”, and “High” (shown by different
724 colours and patterns) correspond to samples after conditioning at low (33%),
725 medium (52%) and high (75%) relative humidity.

726 Figure 3 $\tan \delta$ of the different starch-based films (top: G80; bottom: RMS). “L”, “M”,
727 and “H” (shown by different colours) correspond to samples after conditioning
728 at low (33%), medium (52%) and high (75%) relative humidity.

729 Figure 4 TGA results of the different starch-based films. “L”, “M”, and “H” (shown by
730 different colours) correspond to samples after conditioning at low (33%),
731 medium (52%) and high (75%) relative humidity.

732 Figure 5 Electrical conductivity of the different starch-based films. The error bars
733 represent standard deviations. “Low”, “Medium”, and “High” (shown by
734 different colours and patterns) correspond to samples after conditioning at low
735 (33%), medium (52%) and high (75%) relative humidity.

736

737 **Tables**

738 Table 1 Samples codes, formulations, and relative humidity during conditioning, of the starch-based films.

Code	Formulation ^a					Conditioning
	Starch type	Starch content ^b	[Emim][OAc] content	Water content (original) ^c	Water content (post-conditioning)	Relative humidity (%)
G80-9-L	Gelose 80	85.9	9	35.1	7.60±0.29 ^d	33
G80-9-M		85.9	9	35.1	11.35±0.18	52
G80-9-H		85.9	9	35.1	14.22±0.20	75
G80-18-L		85.9	18	26.1	7.36±0.18	33
G80-18-M		85.9	18	26.1	12.88±0.12	52
G80-18-H		85.9	18	26.1	20.12±0.16	75
G80-27-L		85.9	27	17.1	8.94±0.08	33
G80-27-M		85.9	27	17.1	17.16±0.14	52
G80-27-H		85.9	27	17.1	27.94±0.24	75
RMS-9-L	Regular maize starch	85.6	9	35.4	8.34±0.05	33
RMS-9-M		85.6	9	35.4	11.78±0.27	52

RMS-9-H	85.6	9	35.4	14.87±0.25	75
RMS-18-L	85.6	18	26.4	8.00±0.11	33
RMS-18-M	85.6	18	26.4	12.35±0.11	52
RMS-18-H	85.6	18	26.4	20.69±0.08	75
RMS-27-L	85.6	27	17.4	9.04±0.08	33
RMS-27-M	85.6	27	17.4	15.96±0.22	52
RMS-27-H	85.6	27	17.4	27.84±0.06	75

739 ^a Portions in weight; ^b Dry weight; ^c Combination of added water and original moisture content in starch; ^d Standard deviation

740

741 Table 2 XRD and ¹³C CP/MAS NMR results of the starch-based films

Sample	XRD Results			¹³ C CP/MAS NMR Results			
	Double helix	V-type	Amorphous	Double helix	V-type	Rigid amorphous	Mobile amorphous
Native G80	32.2	ND ^a	–	–	–	–	–
G80-18-L	22.4	8.4	69.2	20.0	10.8	41.6	27.6
G80-18-M	18.4	9.4	72.2	17.5	10.3	46.3	25.9
G80-18-H	21.2	8.2	70.5	20.4	9.1	48.6	21.9
Native RMS	39.5	ND ^a	–	–	–	–	–
RMS-18-L	19.7	4.8	75.5	17.7	6.8	60	15.5
RMS-18-M	18	4.8	77.2	15.9	6.9	57.1	20.1
RMS-18-H	18.4	5.1	76.5	17.5	6.0	57.9	18.6

742 ^a Unable to be determined as the V-type crystallinity pattern was difficult to be differentiated from the A or B-type crystallinity pattern

743

744 Table 3 Glass transition temperatures (T_g) of the starch-based films

Sample	T_g (°C)
G80-18-L	79
G80-18-M	63
G80-18-H	52
G80-27-L	57
G80-27-M	52
G80-27-H	49
RMS-18-L	76
RMS-18-M	73
RMS-18-H	59
RMS-27-L	61
RMS-27-M	56
RMS-27-H	58

745